

Analysis of Elastic Stress Wave Propagation in Stepped Bars, Transmission, Reflection, and Interaction: Experimental Investigation

F.Y. Fraige^{1,2*}, M.H. Es-Saheb²

¹ College of Engineering, Al-Hussein Bin Talal University, P.O. Box 25, Ma'an 71111, Jordan

² Applied Mechanical Engineering Department, College of Applied Engineering, King Saud University, Muzahimiyah Campus, P.O. Box 800, Riyadh 11421; Kingdom of Saudi Arabia

Received 27 OCT 2020

Accepted 31 JAN 2022

Abstract

The behaviour of stepped bars of different materials when impacted longitudinally by mild sphere of different radii was investigated. The passage (or propagation) of the longitudinal stress wave, created from the impact, from one end to another was recorded by strain gauges positioned at various stations along each bar. Different bar combinations with Lagrangian (material) and Eulerian (geometrical) discontinuities were investigated both experimentally and theoretically. Space – time diagrams which demonstrate the stress wave traversals across the discontinuity were constructed. The theoretical analysis of stress wave propagation in solids using the well-established Rayleigh acoustic equations assuming plane sections remain plane, was discussed, and the results were compared well with the experiments.

It was noted that a pulse travelling along a bar with a discontinuity, either in cross sectional area or material difference, will be subjected to amplification or attenuation as it passed through this discontinuity. The amount of change in amplitude was governed by the impedance ratio of the input to output bars. However, the reflected part of the pulse from the discontinuity was always attenuated, with the pulse sign governed by the impedance ratio.

© 2022 Jordan Journal of Mechanical and Industrial Engineering. All rights reserved

Keywords: stress wave; impedance; propagation; bar composites; acoustic impedance.

1. Introduction

Different types of materials and composites are used in systems and structures designed to sustain both static and dynamic load environments. The assessment and prediction of the response of those systems to complex loading conditions are crucial. The study of waves in solids aids in estimating the magnitude of stress created by impact or collision of bodies. Hence, a sound knowledge of elastic stress wave propagation in solids is important for a clear understanding of the impact phenomena and some types of fractures, such as 'spallation' and 'scabbing'. In elastic region, once a material is loaded, it deforms in a completely reversible manner. The behaviour of the material is defined by linear elastic constitutive laws, Hooke's law. This facilitates solving most dynamic problems in the elastic regime analytically. Therefore, the theories on elastic wave propagation in solids are mostly fully developed [1,2].

Stresses caused from intermediate and dynamic loading rates with strain rates in the range of $10 - 10^4$ /s) are transmitted in solids by elastic stress waves [3]. Two types of these waves exist either longitudinal or torsional. The longitudinal stress waves transmit tensile and compressive stresses with speed $C_L = (E/\rho_0)^{1/2}$, which equals the acoustic speed, whereas the torsional waves transmit shear

stresses with speed $C_T = (G/\rho_0)^{1/2}$, where E is the modulus of elasticity, ρ_0 is the density, and G is the modulus of rigidity of the solid material. A stress wave is transmitted through a body when different parts are not in equilibrium, as the case when one solid impinges another. This instability needs finite time to be felt by other parts of the body due to material properties. This is related to characteristic speeds of wave propagation. In longitudinal waves (or sometimes called compressional waves), the individual particles of the bar are displaced or move in the same direction, in case of compression waves, or opposite direction of wave travel in case of tensile wave. While, in torsional waves (or sometimes called shear waves), the particles of the solid are displaced or oscillate entirely in a plane which is transverse to the direction of the wave travel. It is well known that the longitudinal stress waves, both the compressional and tensile are transmitted through the body, while the shear torsional stress waves, known as Love waves, are mainly transmitted on the surface. This explains why these surface shear Love waves are responsible for the most damage associated with the earthquakes and seismic activities. Thus, they attain particular interest in civil engineering, and constitute main criteria for safe engineering designs.

In this paper, an attempt is made to address some issues related to stress wave propagation in longitudinal bars with particular emphasis on the experimental measurements and

* Corresponding author e-mail: Dr.feras@ahu.edu.jo.

analysis of the well-established problem of stress wave propagation in bars with geometrical and materials discontinuities. Thus, the problem of stress wave propagation in solids, particularly in long 'composite' bars, is theoretically and experimentally investigated. This includes the measurement of transmission, reflection, and interaction of the stress waves. The well-established Rayleigh acoustic equations are also given and discussed. The amplification of the stress level during its transmission and reflection in bars with different materials and geometrical discontinuities are also given and discussed. Thus, the behaviour of stepped bars of different materials when impacted longitudinally by mild steel sphere of different radii is particularly investigated. The useful applications of these waves are presented and discussed. Finally, the impact contact times for the various steel spheres and different bars are both experimentally and theoretically investigated. The structure of this work is organized as follows: relevant literature review is outlined in Section 2. The theoretical formulations and analysis of elastic stress wave propagation in long bars is outlined in Section 3 and the Appendix. Section 4 illustrates the apparatus and experimental techniques used, while Section 5 summaries the results and discussion. Finally, Conclusions and future prospects are summarized in Section 6.

2. Literature Review

The existence of sound waves and stress waves which are governed by similar equations and speeds as acoustic waves was recognized early by Rayleigh [4] and introduced after that by Sears[5], who determined the sonic velocity of the bar material using the reflection of stress wave of two ballistically axial impacted bars. Also, Hopkinson who worked on the interaction of incident and reflected waves in collided solids has described a simple technique that enables him to measure both the duration and the maximum pressure developed by an impact [6–8]. Then, his apparatus was further developed and used to establish the general form of an incident compressive pulse caused by impact of a high-speed projectile of different geometrical shapes and materials or from an explosive charge to investigate the behaviour of materials under high strain rates [9–10], and ever since was known as Hopkinson pressure bar and employed by a huge number of investigators. Amongst the large recent research deploying such a device the notable work published by Shin et al [11], who investigated numerically the characteristics of the stress pulse generated by impact of a hollow striker on the flange of a split Hopkinson tension bar. Also, stress transfer mechanism is highlighted by different flange lengths using explicit finite element analysis [12]. Furthermore, particle velocity and stress in the striker and bar generated by the striker impact on a bar with different general impedance based on one-dimensional assumptions is formulated [13].

However, after the early published detailed work by Kolsky [14] and Rinehart and Pearson [15] on waves propagation and analysis, the utilization of stress waves in engineering applications began in the early 1960s by the development of high energy rate forming processes and the uprising of space vehicles and later for determining the

mechanical properties of materials under intermediate and high strain rate loading [1,16–24].

The propagation of a longitudinal compressive stress pulse has been considered early by [9] who employed Hopkinson bar to measure the pressure produced by detonation of the explosive at its end and deduced a mathematical expression for determining the momentum associated with the pulse. Then, several attempts were made to investigate the effects associated with stress waves in rods of varying cross section [10,14,15,18], and in multi-layered plates [20,25,26]. Meanwhile, Zaid investigated the effect of stress waves in a conical bar and developed a computer program to calculate the transmitted and reflected pulses together with their interaction at any section along the bar[18]. Hascoët et al solved numerically the propagation of a shock wave in a chain of elastic beads without restoring forces under traction[27]. Later, Boaratti and Ting employed stress waves propagation sensors along pressurized tubes to detect leakage [28]. Then, Sharma studied the effect of initial stresses on the reflection of stress waves at the free surface of the medium [29]. He observed that the effect of the initial stress on the reflected waves varies with the direction of the incident wave, the elastic properties, and the anisotropy present in the material.

Recently, many new industries, such as communication, energy, automobile, aircraft, and space are expanding rapidly and striving to use increasing new materials including composites, metal matrix composites, piezoelectric materials, functionally graded material (FGM), powder compacts and superplastic materials, ceramics, and nano powders. The adoption of such newly developed materials and fast manufacturing techniques and protection against shock loadings initiated huge interest and research work on dynamic properties of these materials and structures, and further research on these newly produced materials to be shaped and formed into their final shape as to become traditionally used [30–32].

Stresses and strains developed in FGM subjected to quasi-static loading were estimated by Suresh et al [33,34]. They highlighted that by optimizing the structure and geometry of the graded interface between the two dissimilar layers, the stress levels are significantly reduced. Li et al investigated the response of plates made of metallic ceramic in two dimensions [35]. While Han et al extended the problem to three dimensions and the effect of impact was numerically investigated [36]. The FGM investigated is approximated to a multi-layered structure with uniform material properties of each layer. Then, the propagation of stress waves in FGMs using a composite wave propagation algorithm was numerically studied by Berezovski et al [37,38]. They observed that the size, shape, clustering, and in homogeneities in the random distribution of embedded reinforcement particles may affect the results of simulation of the model they proposed. Earlier, Twofighi et al examined the elastic wave propagation in the circumferential direction of anisotropic cylindrical curved plates [39]. They used Fourier series expansion technique to facilitate solving the wave propagation problem. Tasedemirics et al used split-Hopkinson pressure bar to investigate the high strain rate compression on multilayer materials [40]. The viability of modelling stress wave propagation in complex multilayer

materials has been demonstrated. They have shown that the effects of lateral confinement of a normally low-modulus interlayer material can affect the response wave propagation significantly. Xu and Rosaki assessed the generation and subsequent evolution of impact damage in heterogeneous two layered materials: one is a polymer layer which bonded to a second metallic layer when subjected to impact loading. High speed photography and dynamic photo elasticity were utilized to visualize the nature and sequence of dynamic failure modes [41]. Meanwhile, Gebbeken and Greulich developed a three-dimensional dynamic model to investigate the stress wave propagation in a reinforced concrete bar. As expected, the mechanical behaviour was characterized by cracking of the concrete [42]. However, using modified smoothed particle hydrodynamics (MSPH) method, Zhange and Batra investigated the elastic wave propagation in FGMs [43]. They showed that for the same placement of particles, the MSPH method gave better results comparing with the finite element method. But, in a later work, Perez and Al-Haik employed a one-dimensional impact problem for a layered system that comprises heterogeneous materials with different geometrical configurations [44]. They tracked the stress wave propagation using analytical model. The results showed that layered systems suffered stress amplification with inherent acoustic impedance mismatch between layers. The effect of discontinuities on the wave propagation characteristics of structures is investigated by Rafiee-Dehkharghani et al [21]. They proposed new architectures for attenuating stress waves. Due to the highly nonlinear nature of the optimization problem combined with lack of gradient information about the objective function with respect to design variables, a genetic algorithm optimization procedure was used for the optimal design of the newly defined attenuating systems.

Working on materials modelling, Ogden and Singh derived the general constitutive equation for a transversely isotropic hyper-elastic solid in the presence of initial stress based on the theory of invariants [45]. They claimed that the speed of homogeneous plane waves and surface waves depend nonlinearly on the initial stress, in contrast to the situation of the more specialized isotropic and orthotropic theories of Biot. The speeds of homogeneous plane shear waves and Rayleigh waves in an incompressible material were obtained and they noticed that significant differences from Biot's results for both isotropic and transversely isotropic materials with calculations based on a specific form of strain-energy function. Also, Barzkar and Adibi proposed a generalized Kelvin-Voigt model of viscoelasticity with the aim of bridging the gap between solids and fluids leading to a new concept of viscoelasticity which unifies the Navier-Lame and the Navier-Stokes equations [46]. On solving this equation in one dimension, propagation of stress disturbance in the so-called "Kelvin-Voigt materials" was studied. The model of these materials enabled them to investigate all the elastic and viscoelastic solids, as well as fluids and soft materials. Also, Walley and Field summarized the difference between ideal and real elastic materials [22]. They showed the dissipation mechanisms which cause attenuation of elastic waves with distance travelled. This rate of attenuation usually depends on frequency.

Recently, Ebrahimi et al reviewed mechanical, thermal, and electrical properties of nanostructures that exhibit piezoelectric behaviour including wave propagation [47]. Later, the bending of magneto-electric-elastic nanobeams and its relationship with nonlocal elasticity theory is studied [48]. Furthermore, Singhal et al investigated analytically Love-type wave vibrations in a distinct piezoelectric material thin film with a highly and weakly dielectric interface with an elastic pre-stressed plate [49]. Also, in a recent publication, Singhal and co-investigators examined Love-type wave transmission through compressive stressed orthotropic substrate welded on couple stress half-space with imperfect interface [50]. Meanwhile, Saroj et al studied the Love-type wave propagation in irregular functionally graded piezoelectric material resting over elastic half-space with irregular boundary [51].

It is important to state that despite the vast amount of work and published research, over the last few decades, in impact mechanics and stress wave propagation in materials and structures; the main efforts were clearly concentrated on the theoretical studies, simulation, numerical and modelling approaches. Hence, relatively little of this important research effort is directed to experimental investigation of this problem. This is clearly reflected in the scant experimental research works found and published.

Therefore, in this work an attempt is made to address some of these issues with particular emphasis on the experimental measurements and analysis of the well-established problem of stress wave propagation in bars with geometrical and materials discontinuities. Thus, the problem of stress wave propagation in solids, particularly in long 'composite' bars, is theoretically and experimentally investigated.

3. The Theoretical Formulations and Analysis

As stated above, the theoretical analysis of elastic stress wave propagation in long bars is very well known and established in literature. However, for convenience and benefit completion a brief summary of the most related theoretical analysis of this problem is presented [3,18]. The main equations and relations concerned are addressed and documented in the Appendix.

4. Apparatus and Experimental Techniques

The experimental setup, shown in Fig.1-a, consists of a frame(1), pendulum sphere with various radii (2), bar specimen (3), strain gauges, oscilloscope (4), amplifier, power source (5), and camera (6). The frame which is made up of two horizontal beams supported on four stands, was used to hang the test specimens in a free horizontal position. Strain pulse was produced by impacting a steel sphere supported from one end of the frame as a simple pendulum against the plane surface of the test bars. Fine adjustments for the height of the sphere were provided by two screws attached to the two beams of the frame as shown in Fig.1-b. These adjustments were necessary to ensure that the sphere impacts the test bar at the centre of its cross-sectional area.

The pulses, thus produced, were recorded using strain gauges connected at a predefined station on both the input and output bars as shown in Fig.1-c (block diagram). The strain gauges were attached diametrically opposite to the bars and connected as the active arms of the measuring Whitestone bridge. This arrangement of strain gauges eliminates bending strains and gives twice the sensitivity of that signal obtained using a single active gauge. The output of the bridge is displayed on a dual beam Tektronix

oscilloscope and then photographed using a Polaroid camera, for later processing, analysis and calculation.

The complete specifications and details of the three steel spheres used in this investigation together with the bar's combination specimens of different geometries and materials (i.e. Steel, Brass and Aluminium) are shown in Table 1, and Table 2-a, b and c respectively. Typical tapered bar specimens are shown in Fig.2-a and stepped bars specimens in Fig.2- b.

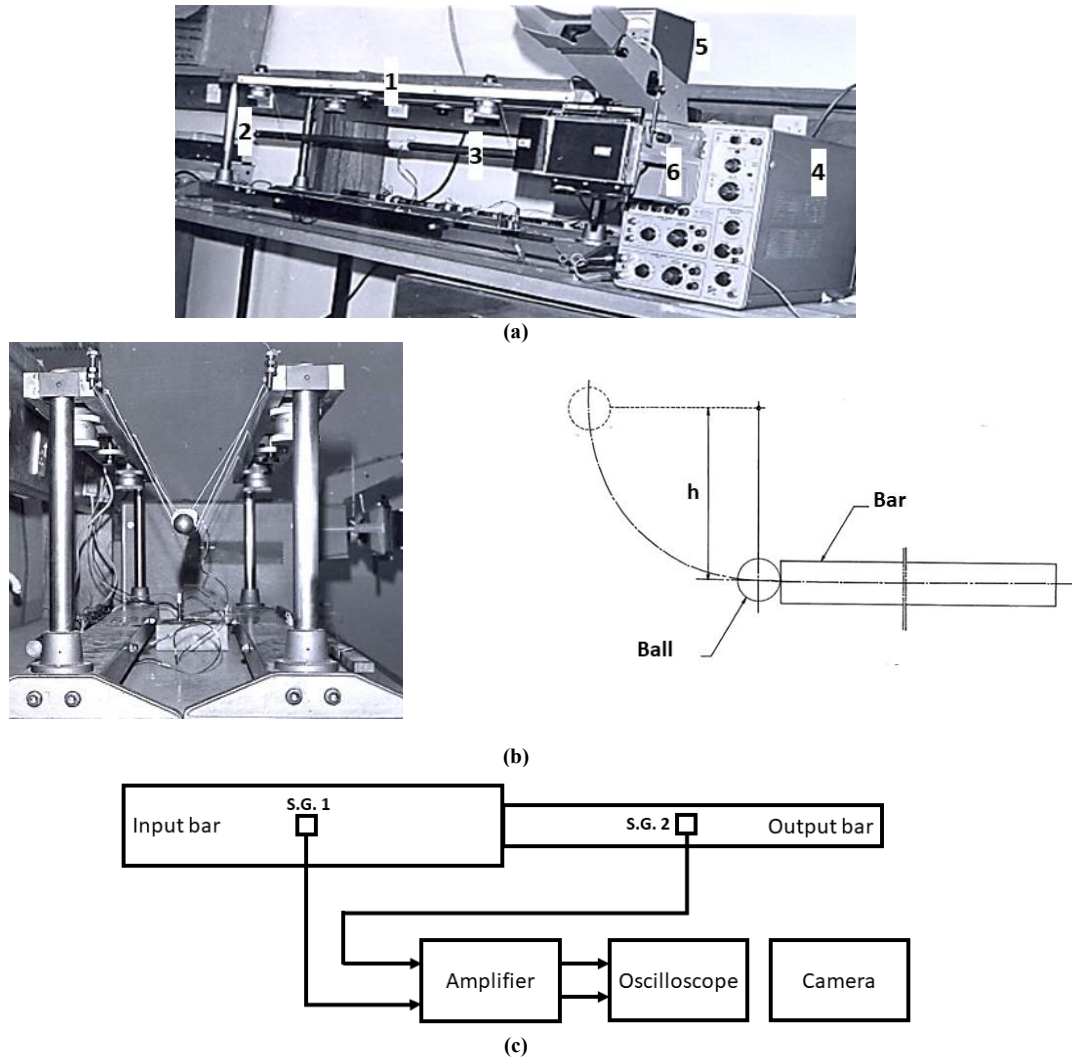


Figure 1. Experimental setup (a) Picture; shows: (1) Frame, (2)Steel sphere, (3)Rod specimen, (4) Oscilloscope, (5) DC power supply and (6) Camera; (b) Pendulum arrangement; and (c) A schematic block diagram.

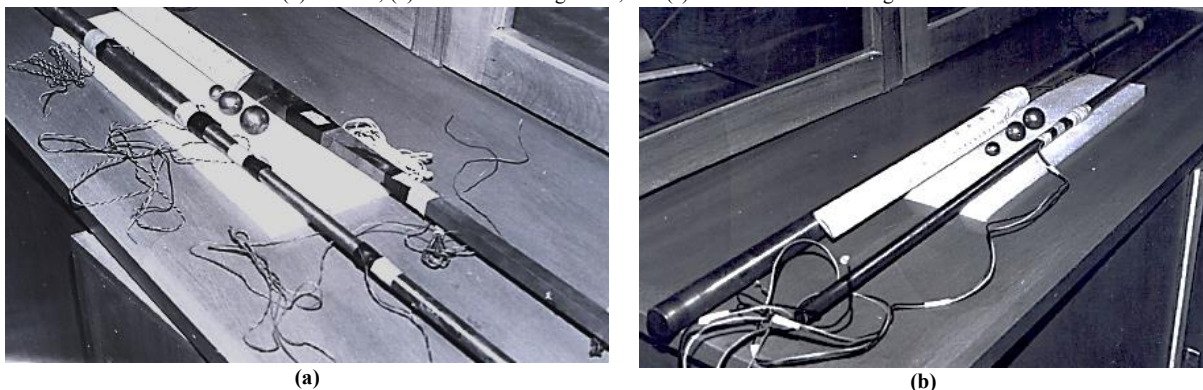


Figure 2. Tapered steel specimen; (a) Linear (rectangular and circular cross sections) and (b) Typical circular stepped steel bar specimen (circular cross sections).

Table 1. The complete details and specifications of the steel spheres used.

Sphere No.	Sphere diameter d_s , mm (in)	Sphere Mass m_s , gram (lb)
1	25.4 (1)	67.74 (0.1492)
2	22.23 (0.875)	45.49 (0.1002)
3	15.88 (0.625)	17.16 (0.0378)

Table 2. The complete details and specifications of the experimental bar specimens used.

Table 2-a. Bars combinations specimen number 1 - 10.

Sp. No.	Material	Steps No.	Diameter mm (in)	Length mm (in)	Mass kg (lb)	Remarks
1	Steel	0	25.4 (1.000)	1000 (39.37)	3.980 (8.767)	See Fig. 2-b $\rho_o = 7805.73 \text{ kg/m}^3$ (0.282 lb/in ³)
2	Steel	0	12.7 (0.500)	1000 (39.37)	1.005 (2.214)	See Fig. 2-b
3	Brass	0	12.07 (0.475)	971.55 (38.25)	0.935 (2.059)	$\rho_o = 8553.1 \text{ kg/m}^3$ (0.309 lb/in ³)
4	Brass	0	20.01 (0.788)	1249.93 (49.21)	3.310 (7.291)	-
5	Brass	0	28.68 (1.129)	1258.82 (49.56)	6.770 (14.912)	-
6	Aluminium	0	20.01 (0.788)	1257.3 (49.5)	1.085 (2.390)	$\rho_o = 2643.43 \text{ kg/m}^3$ (0.0955 lb/in ³)
7	Aluminium	0	25.02 (0.985)	1244.6 (49)	1.652 (3.639)	-
8	Steel + Steel	1	25.4 (1.000)	-	-	Single stepped bar
			12.7 (0.500)	-	-	$\rho_o = 7805.73 \text{ kg/m}^3$ (0.282 lb/in ³)
9	Brass + Brass	1	28.68 (1.129)	-	-	Single stepped bar
			12.07 (0.475)	-	-	-
10	Aluminium + Brass	0	20.01 (0.788)	-	-	Composite bar
			20.01 (0.788)	-	-	-

Table 2-b. Steel circular tapered bar specimen number 11.

Sp. No.	Material	Large diameter d_1 mm (in)	Small diameter d_2 mm (in)	Length mm (in)	Remarks
11	Steel	24.13 (0.95)	12.19 (0.48)	1244.6 (49.0)	See Fig. 2-a

Table 2-c. Steel rectangular tapered bar specimen number 12.

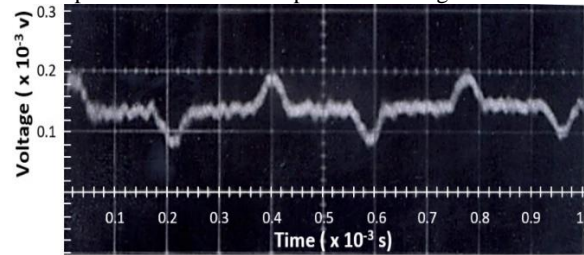
Sp. No.	Material	Thickness mm (in)	Larger width w_1 mm (in)	Smaller width w_2 mm (in)	Length mm (in)	Remarks
12	Steel	12.95(0.51)	25.91 (1.02)	12.95 (0.51)	1283.2 (50.52)	See Fig. 2-a

4.1. Specimen joining Method

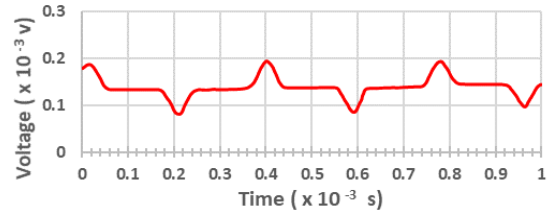
Stepped and composite bars combinations specimen numbers 8,9 and 10 (see Table 2-b), were fabricated by cementing the two bar elements together using Araldite cement. Tensile tests were carried out to determine the strength of bonds thus obtained. To separate a test specimen composed of two 25mm (1.0 in) dia. steel bars a force of 6.00 KN (1350 lb) was needed. This corresponds to a stress of 11.75N/mm² (1700psi), which is much higher than those anticipated stresses induced in the specimen during actual test conditions. The method of joining the specimens in this manner proved satisfactory and was used throughout the work.

5. Results and Discussion

Many oscilloscope traces were photographed showing stress wave propagation in the various test bars. A photograph illustrates a typical strain signal, obtained for a 25mm dia. steel bar impacted with 21.875mm (7/8 inch) dia. steel sphere is displayed in Fig. 3-a. However, all tests signals were retraced and manipulated with a digitizing signal software, and transformed to digital signal forms for further processing and calculations. Of these, five representative traces are presented in Figs. 4 to 8.



(a)



(b)

Figure 3. A typical strain signal obtained for a 25.4mm (1-inch) diameter steel bar of 984.25mm (39.37 in) length impacted with a 21.875mm (7/8 inch) diameter steel sphere; (a) A photograph; and (b) Digital signal form.

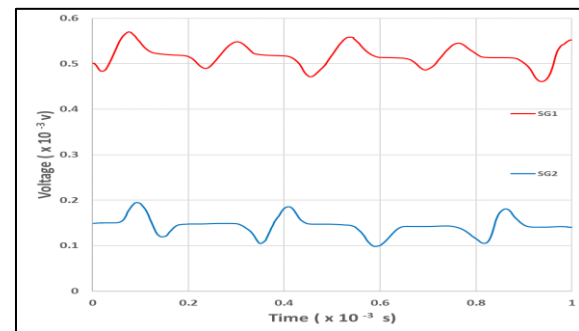


Figure 4. Strain-Time trace, for a one -step Steel bar, with area ratio $A_1/A_2 = 4$.

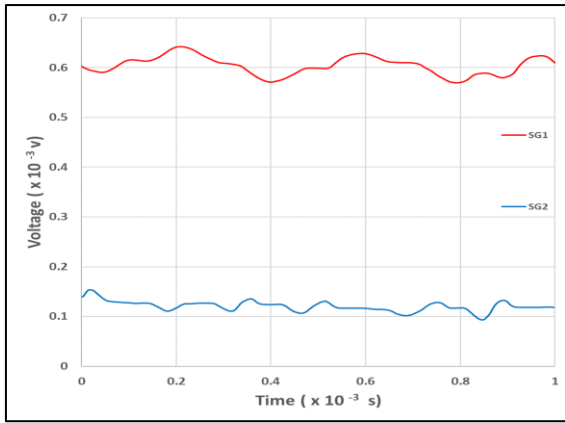


Figure 5. Strain-Time trace, for a one -step Brass bar, with area ratio $A_1/A_2 = 5.649$.

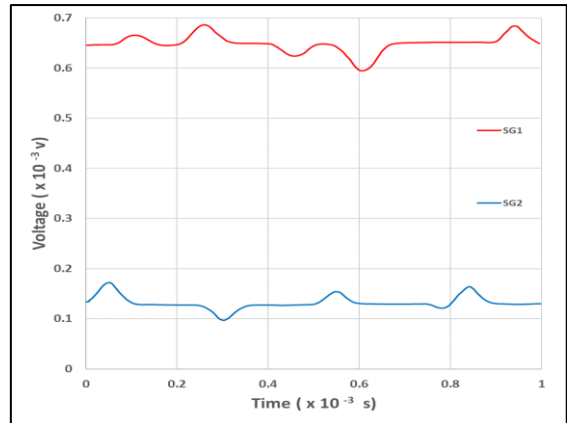


Figure 6. Strain-Time trace, for a composite bar of Aluminium and Brass, with area ratio $A_1/A_2 = 1$.

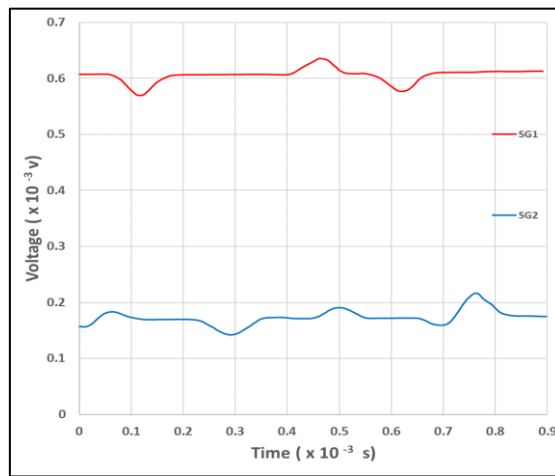


Figure 7. Strain-Time trace, for a composite bar of Brass and Aluminium, with area ratio $A_1/A_2 = 1$.

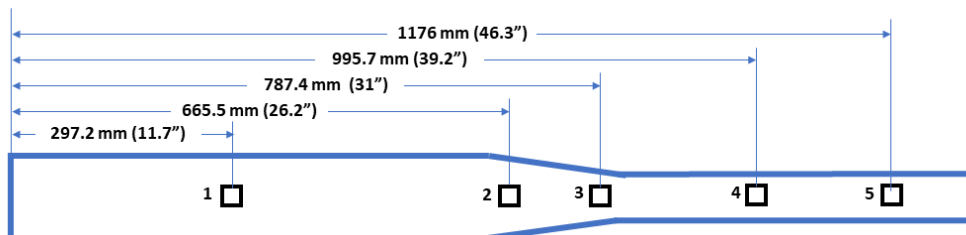
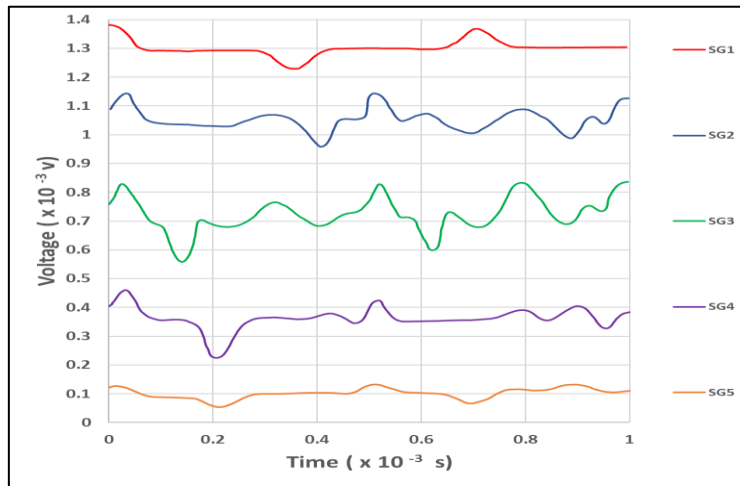


Figure 8. Strain-Time trace, for Steel tapered bar shown.

The theoretical and experimental values of the longitudinal wave speeds C_L and the Young's modulus E are calculated for the different bar materials specimens and displayed in Tables 3. The absolute relative error is less than 1.5% and 2.2% for wave speed and Young's modulus, respectively.

Table 3. The theoretical and experimental values of the longitudinal wave speed and Young's modulus for Steel, Brass and Aluminium specimens.

Sp. No.	Material	Theoretical Stress wave speed, C_L at 0° C, m/s (ft/sec.)	Experimental Stress wave speed, C_L at 25° C, m/s (ft/sec.)	Youngs Modulus, E, GPa (psi)	Experimental Youngs Modulus, E, GPa (psi)
1&2	Steel	5151 (16900)	5128 (16824)	203.4 (29.5x10 ⁶)	205.5 (29.8x10 ⁶)
3,4 &5	Brass	3352 (11000)	3401 (11160)	93.08 (13.5x10 ⁶)	95.15 (13.8x10 ⁶)
6&7	Aluminium	5090 (16700)	5102 (16740)	68.95 (10x10 ⁶)	69.64 (10.1x10 ⁶)

Also, the experimental values of the transmitted and reflected stress are calculated and displayed in Table 4 for the stepped steel, brass and composite (Aluminium and brass) bars. Meanwhile, the secondary transmitted stress (σ^T , σ^{T^2} , and σ^{T^3}) and reflected stress (σ^R , σ^{R^2} and σ^{R^3}) values for the steel and brass stepped specimens are shown in Table 5.

σ^{R^2} , σ^{R^3}) values for the steel and brass stepped specimens are shown in Table 5.

Table 4. The transmitted and reflected stress values in the stepped steel, brass and composite (Aluminium and brass) bars.

Sp. No.	Step Ratio A_1/A_2	Transmitted stress wave, σ_T	Reflected stress wave, σ_R	Remarks
8	4	1.6 σ_1	-0.6 σ_1	See Fig. 4
9	5.649	1.7 σ_1	-0.7 σ_1	See Fig. 5
10	1	1.36 σ_1	0.36 σ_1	See Fig. 6
		0.639 σ_1	-0.361 σ_1	See Fig. 7

Table 5. The secondary transmitted and reflected stress values in the steel and brass stepped bars.

Sp.No.	σ^T	σ^R	σ^{R^2}	σ^{T^2}	σ^{R^3}	σ^{T^3}	Remarks
8	1.6 σ_1	0.6 σ_1	-0.96 σ_1	-0.64 σ_1	0.58 σ_1	0.38 σ_1	See Fig. 8
9	1.7 σ_1	-0.7 σ_1	-1.2 σ_1	-0.5 σ_1	0.84 σ_1	0.38 σ_1	

Also, the results of the typical theoretical and experimental stress values of the transmitted and reflected stress wave passage (i.e. with time history), as well as the experimental detection times of the stress signals for stepped and composite bars, are calculated and shown in Tables 6 and 7 respectively.

Table 6. Typical theoretical and experimental stress values of the transmitted and reflected stress wave passage (i.e with time history) in stepped Steel, brass and composite (aluminium and brass) bars.

Theoretical Results			Experimental Results		
Time at reflection x 10 ⁻³ sec.	σ_R/σ_I	Detective time x 10 ⁻³ sec.	Time at reflection x 10 ⁻³ sec.	σ_R/σ_I	Detective time x 10 ⁻³ sec.
Steel Bar (Sp. No. 1)					
0.189	-1	0.0945	0.190	-1.00	0.09
0.378	+1	0.2835	0.380	+1.00	0.28
0.567	-1	0.4725	0.540	-1.10	0.47
0.756	+1	0.6615	0.760	+1.10	0.64
0.945	-1	0.8505	0.950	-0.96	0.85
Brass Bar (Sp. No. 4)					
0.373	-1	0.1865	0.340	-0.964	0.12
0.746	+1	0.3917	0.670	+0.923	0.43
1.119	-1	0.7647	1.100	-0.980	0.78
Aluminium Bar (Sp. No. 6)					
0.247	-1	0.1235	0.260	-1.00	0.12
0.494	+1	0.3705	0.460	+0.91	0.36
0.741	-1	0.6175	0.720	-1.12	0.63
0.988	+1	0.8645	0.940	+0.98	0.84

Table 7. Typical experimental detection times of the stress signals for stepped and composite bars.

Experimental Reflecting Time x 10 ⁻³ sec.		Experimental Detective Time x 10 ⁻³ sec.	
t	t''	T ₁	T ₂
a) Steel Stepped Bar (Sp. No. 8)			
0.16	0.24	0.00	0.06
0.38	0.50	0.20	0.31
0.61	0.70	0.41	0.54
0.84	0.93	0.64	0.56
b) Brass Stepped Bar (Sp. No. 9)			
0.12	0.10	0.00	0.00
0.30	0.25	0.13	0.16
0.50	0.40	0.33	0.29
0.68	0.61	0.52	0.46
0.85	0.82	0.72	0.65
c) Brass and Aluminium Composite Bar (Sp. No. 10)			
0.00	0.18	0.07	0.02
0.31	0.40	0.38	0.22
0.54	0.60	0.54	0.43
0.78	0.88	0.90	0.64

Furthermore, the theoretical and experimental values of the transmitted/incident and reflected/incident stress ratios at the discontinuities are calculated at a typical selected time applying Eqs. (9 and 10) and shown in Table 8. This, also, is assessed by Fig.9, which displays a constructed typical space-time diagram for a composite bar (Brass and Aluminium).

Experimental results show that nearly all recorded signals follow much the same pattern. This is because the local velocity of the elements transmitting the wave depends on the form of the disturbing force, which is affected by the geometrical shapes of the impacted bodies and the manner of applying the impact. In our case, mild steel sphere supported as a pendulum is used to produce the impact force in all tests, hence the signals obtained are of the same form.

In general, the shape of the recorded pulses is influenced by the relative values of specimen length (l) and pulse length (λ), as shown in Fig. 10. When $\lambda < l$ as shown in Fig. 10 a, the incident pulse is registered before

the wave front of the reflected pulse arrives back at the strain gauge location. The incident and reflected pulses are recorded separately and no over-lapping occurs (see for example Fig.3). A critical case arises when $\lambda=l$. Here, the wave front of the reflected pulse arrives back at the strain gauge location when the tail of the incident pulse is just about to leave the gauge. Finally, $\lambda > l$ is when over-lapping between incident and reflected waves occurs. Thus, the recorded signal will include components of both incident and reflected pulse and the usefulness of the results could be diminished.

To avoid over-lapping, the length of the bar and the axial location of the gauges along the bar must be carefully selected. Initial tests were carried out to determine the wave length of the stress pulse. Based on this, a suitable length for the various bars was chosen. The typical experimental wave length values obtained in steel, brass and aluminium specimens are measured for the various impact conditions and displayed in Table 9.

Table 8. Typical theoretical and experimental values of the transmitted/incident and reflected/incident stress ratios at typical selected times of the stress wave passage for stepped and composite bars.

Time	t_1		t_2		t_3		t_4	
Stress Ratio	σ_R/σ_I	σ_T/σ_I	σ_{R1}/σ_I	σ_{R2}/σ_I	σ_{R3}/σ_I	σ_{R4}/σ_I	σ_{T3}/σ_I	σ_{T4}/σ_I
Case A: One step Steel bar (Sp. No. 8)								
Theoretical	-0.6	1.6	-1.6	0.6	-0.96	-0.36	-0.64	0.96
Experimental	-	-	-1.5	0.7	-0.84	-0.43	-0.57	0.84
Case B: One step Brass bar (Sp. No. 9)								
Theoretical	-0.7	1.7	-1.7	0.7	-1.19	-0.49	-0.51	1.19
Experimental	-0.67	2.0	-2.0	0.59	-1.10	-0.46	-0.60	1.07
Case C: Brass and Aluminium composite bar (Sp. No. 10)								
Theoretical	-0.36	0.640	-0.64	+0.36	-0.13	-0.23	0.23	-0.870
Experimental	-0.34	0.625	-0.62	+0.32	-0.18	-0.25	0.36	-0.875

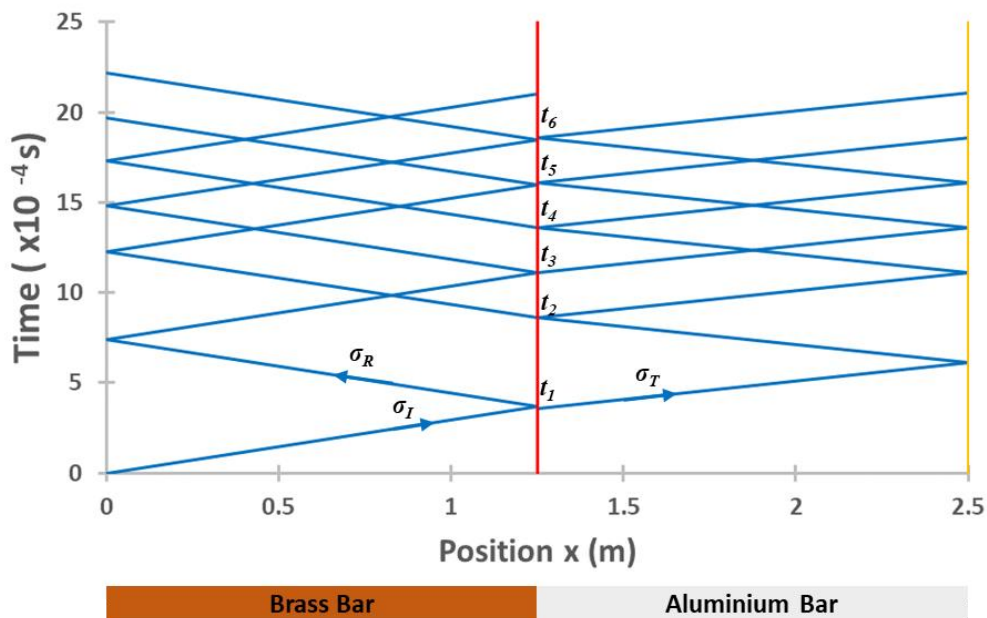


Figure 9. Space-Time diagram for composite Brass and Aluminium bar, with area ratio $A_1/A_2 = 1$.

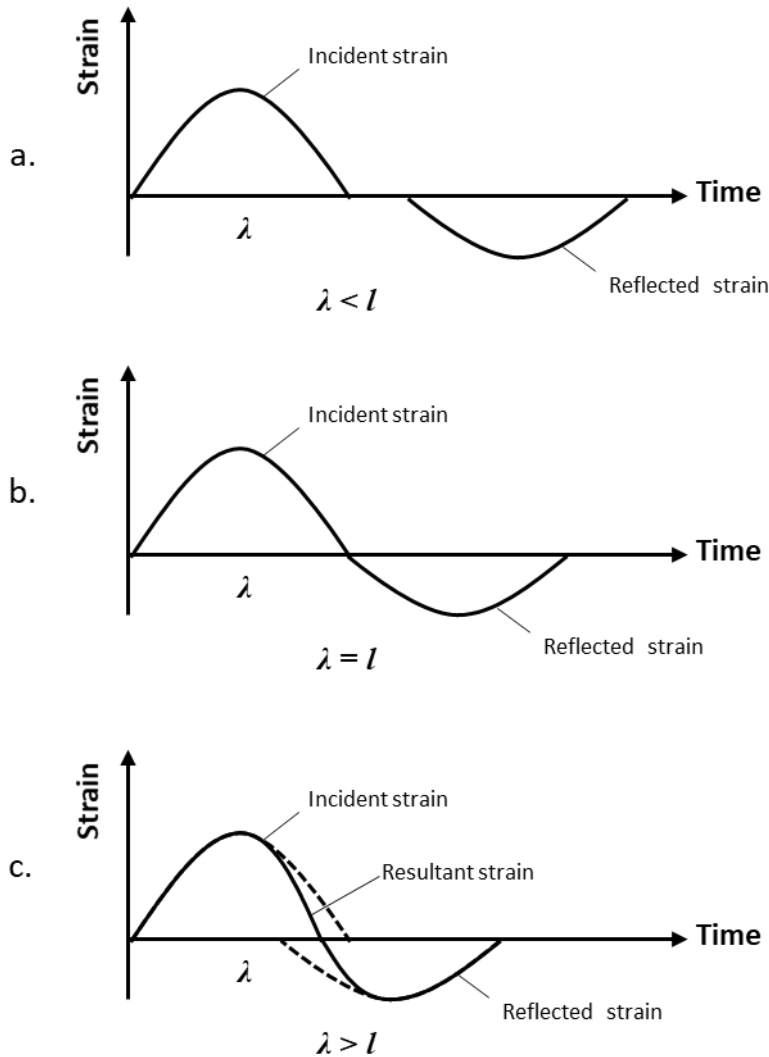


Fig. 10. Predicted wave forms in a stepped bar for different relative values of specimen length, l , and pulse length, λ .

Table 9. Typical experimental wave length values obtained in steel, brass and aluminium specimens.

Sphere Diameter, mm (in)	Wave Length, λ , m (ft)			
	Steel Bar (Sp. No. 1)	Brass Bar (Sp. No. 3)	Brass Bar (Sp. No. 4)	Aluminium Bar (Sp. No. 6)
25.4 (1)	0.732 (2.4)	0.503 (1.65)	0.469 (1.54)	0.61 (2.0)
22.23 (7/8)	0.518 (1.7)	0.402 (1.32)	0.369 (1.21)	0.457 (1.5)
15.88 (5/8)	0.411 (1.35)	0.268 (0.88)	0.274 (0.9)	0.411 (1.35)

The relative values of the incident (σ_i), reflected (σ_R) and the transmitted (σ_T) waves are governed by the mechanical impedance ratio of the input bar to that of the output bar. A very important conclusion can be drawn from this. Consider that a compressive stress wave is applied, for example, to a concrete column. Upon reflection, the wave will become tensile. As concrete is stronger in compression than tension, it is conceivable that the column would fracture in tension even though the amplitude of the initial applied pulse was less than the ultimate strength of concrete in compression. Values of σ_R/σ_i and σ_T/σ_i as measured directly from the records seem in reasonable agreement with the theoretical predictions.

In the theoretical analysis some assumptions have been made such as "plane sections remain plane"; the validity of this assumption is questionable near a discontinuity. The behaviour of the stress waves at the discontinuity is

complicated by local stress waves interactions taking place in the vicinity of the discontinuity. Also, Poisson's ratio and consequently radial inertia have been neglected. In actual situations, the radial vibrations could lead to dispersion of the applied pulse.

The significance of the space-time diagram, see Fig. 9, is that it shows the times when the stress wave passes any axial location along the bar. Values of time read from this diagram at the location of the gauges seem to tie in with the corresponding values on the recorded results. This adds weight to the accuracy of the experimental results.

When bars of different materials of the same length are impacted with the same sphere, the signals produced are almost the same in shape, but differ in amplitude and wave length, depending on the properties of the materials, and the wave speed in each, as illustrated in Figs. 3-8. It was noticed, also, that when a bar is impacted with spheres of

different diameters, the larger sphere gives longer contact time. Hence, values of the contact time between the impinging sphere and the end of the bar was calculated and found to be in good agreement with those measured from the length of the pulse. The details of the mechanics of elastic spheres impact based on the Hertz problem analysis including the main equations used for calculation of the contact times are shown in the Appendix. Thus, the theoretical and experimental contact times plotted against the radii of the three impacting spheres, are shown in Fig. 11.

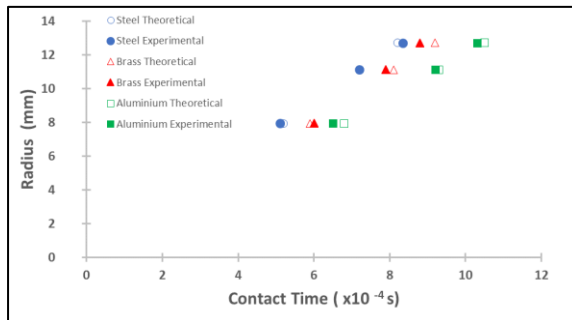


Figure 11. Theoretical and experimental variation of contact time with sphere radii for Steel, Aluminium and Brass bars.

The apparatus used was simple and could be upgraded with little effort. Some difficulties were, however, experienced in recording the signals. At first, there was a large amount of noise superimposed on the signal. This was partly solved using differential amplifiers and appropriate earthing of the system. In this manner most of the noise was suppressed and the signal/noise ratio was increased to an acceptable level. Another problem was associated with the triggering of the oscilloscope. The method adopted was to utilise the initial strain pulse to trigger the beam. This resulted in the loss of an essential part of the first pulse. These problems may be overcome with the use of more sensitive gauges (e.g. semi-conductor strain gauges) and the use of external triggering system.

Finally, the study of the impact stresses and the phenomena of stress waves in solids is of great value due to its wide applications. In fact, there are many occasions in engineering design where some components are subjected to impact loads or various impact fractures, such as spalling and scabbing (i.e. Fractures of bars and plates due to stress wave reflections), which are difficult to explain without the knowledge of the stress wave behaviour. Thus, stress wave aspects are widely used in military, machine element design and load sudden release applications. Extended studies of the different bar's configurations, materials and geometrical shapes including tapered and multi-stepped bars as well as the collinear collision of bars are essential. The design of impact momentum traps is very useful for structure safety.

6. Conclusions

In this work, the theoretical and experimental study of longitudinal stress wave propagation in solid composite bars with various geometrical and material discontinuities is successfully achieved. The stress wave propagation in simple composite bar configuration impacted longitudinally with steel spheres involving geometrical (i.e. tapered and stepped bars) and materials

(steel, aluminium, and brass i.e. composite bars) discontinuities combinations is theoretically evaluated and experimentally measured successfully. The theoretical and experimental values obtained, are found to be in excellent agreement reaching 98% accuracy. The shape of the recorded stress pulse is found to be influenced by the relative values of specimen length (l) and pulse length (λ). It is also, observed that the behaviour of the stress waves at a discontinuity is complicated by local stress waves interactions taking place in the vicinity of the discontinuity. The stress waves trapped and reverberate in the solid setting up wave interference that could produce large transient stresses were confirmed. The values obtained for the relative values of the incident reflected and transmitted waves are proven to be governed by the impedance ratio of the input bar to that of the output bar. The impedance matching condition (i.e. when the impedance ratio is unity) is also observed. Furthermore, the calculated and measured values, of the contact time between the impinging sphere and the end of the bar, based on Hertz analysis, are found to be in excellent agreement.

Finally, these promising results obtained, encourage further investigation on more complex composite structures and various damages and fractures involved in the impact process. A comprehensive theoretical and experimental investigation covering the damages caused by the stress waves and their transmission, reflection, and interaction causing scabbing and multiple scabbing fractures is discussed, recommended, and needed. Furthermore, the order of the composite materials 'cladding' process, which affects these phenomena and fracture mechanisms involved require intensive future research. The design and use of the momentum traps to avoid such fractures is also suggested.

Acknowledgement

The authors extend their appreciation to the Deanship of Scientific Research at King Saud University for funding the work through the research group project no. RGP-VPP-036.

References

- [1] Achenbach J. D., 1975, Wave Propagation in Elastic Solids, Elsevier, ISBN: 0720403251, Netherlands.
- [2] Bedford, A. & Drumheller, D.S., 1994, Introduction to Elastic Wave Propagation, John Wiley & Sons Ltd., West Sussex, England. updated version is available <https://imechanica.org/files/awave.pdf>, accessed 07/09/2019.
- [3] Zaid, A.I.O. 2016, Stress Waves in Solids, Transmission, Reflection and Interaction and Fractures Caused by Them: State of the Art, International Journal of Theoretical and Applied Mechanics, 1, pp 155-164.
- [4] Rayleigh, J.W.S., 1877, Theory of Sound, Vol 1, Macmillan, and Co. London UK.
- [5] Sears, J. S., 1907, On the longitudinal impact of metal rods with rounded ends, Transactions of the Philosophical Society, 21 (2), pp. 49 - 105. <https://www.math.fsu.edu/~agashe/junk2.pdf>.
- [6] Hopkinson B., 1914, A method of measuring the pressure produced in the detonation of high explosives or by the impact of bullets, Philosophical Transactions

- of the Royal Society A, 213, pp. 437 – 456. DOI: <https://doi.org/10.1098/rsta.1914.0010>.
- [7] Hopkinson B., 1914, The effects of the detonation of gun cotton, *Trans. North-East Coast Inst. Eng. And Shipbuilders*, 30, pp. 199.
- [8] Hopkinson B., 1921, The pressure of a blow. In *The scientific papers of Bertram Hopkinson* (eds JA Ewing, J Larmor), pp. 423–437. Cambridge, UK: Cambridge University Press.
- [9] Landon J.W. & Quinney H., 1923, Experiments with the Hopkinson pressure bar, *Proceeding of Royal Society Series A*, 103 (723), pp. 622-643. <https://doi.org/10.1098/rspa.1923.0084>.
- [10] Davies R.M., 1948, A critical study of the Hopkinson pressure bar, *Philosophical Transactions of The Royal Society of London Series A*, 240, pp. 375.
- [11] Shin H, Lee J-H, Kim J-B, & Sohn S-I., 2020, Design guidelines for the striker and transfer flange of a split Hopkinson tension bar and the origin of spurious waves. *Proceedings of the Institution of Mechanical Engineers, Part C: Journal of Mechanical Engineering Science.* 234(1), pp. 137-151. doi:10.1177/0954406219869984.
- [12] Shin H, Kim S, & Kim J-B., 2020, Stress Transfer Mechanism of Flange in Split Hopkinson Tension Bar. *Applied Sciences*, 10(21):7601. <https://doi.org/10.3390/app10217601>.
- [13] Shin H, & Kim D. 2020, One-dimensional analyses of striker impact on bar with different general impedance. *Proceedings of the Institution of Mechanical Engineers, Part C: Journal of Mechanical Engineering Science.*;234(2), pp. 589-608. doi:10.1177/0954406219877210.
- [14] Kolsky, H., 1953, *stress waves in solids*, 1st edition, Oxford University Press [at the Clarendon].
- [15] Rinehart J. S. & Pearson J. 1954, *Behavior of Metals under impulsive loads*, American Society for Metals, Cleveland, Ohio, USA.
- [16] Tsui T.Y., 1968, Wave Propagation in a Finite Length Bar with a Variable Cross Section, *Journal of Applied Mechanics-ASME*, 35(4), 824-825. <https://doi.org/10.1115/1.3601317>.
- [17] Kinslow R., 1970, *High velocity impact phenomena*, 1st edition, Academic press, 1970. <https://doi.org/10.1016/B978-0-124-08950-1.X5001-0>.
- [18] Johnson W., 1972, *Impact strength of materials*, Edward Arnold Ltd., London, UK.
- [19] Zaid, A.I.O. 1997, Effects of Stress Wave Propagation in conical Rods, in *Proceedings of the 5th International Symposium on Advanced Materials (ISAM -5)*, Khan, A.Q. (Ed.), 21st – 25th Sept 1997, pp. 576-581, Doctor AQ Khan Research Laboratories Kahuta Rawalpindi, Pakistan.
- [20] Goldsmith W. & Sackman J. L., 1992, An experimental study of energy absorption in impact on sandwich plates, *International Journal of Impact Engineering*, 12 (2), pp.241–262. [https://doi.org/10.1016/0734-743X\(92\)90447-2](https://doi.org/10.1016/0734-743X(92)90447-2).
- [21] Rafiee-Dehkharghani R., Aref A.J., & Dargush G., 2015, Stress Wave Attenuation in Solids for Mitigating Impulsive Loadings, Technical Report: MCEER-15-0003, ISSN 1520-295X. <http://www.eng.buffalo.edu/mceer-reports/15/15-0003.pdf>.
- [22] Walley S.M. & Field J.E., 2016, Elastic Wave Propagation in Materials, Module in Materials Science and Materials Engineering doi:10.1016/B978-0-12-803581-8.02945-3.
- [23] Sha Y., Dianhao C., & Jun X., 2019, Novel propagation behavior of impact stress wave in one-dimensional hollow spherical structures, *International Journal of Impact Engineering* 134, 103368, <https://doi.org/10.1016/j.ijimpeng.2019.103368>.
- [24] Damamme G., Vermunt J., Pierre Zappa D., & Klöcker H., 2019, Stress release waves in plastic solids, *Journal of the Mechanics and Physics of Solids*, 128, p 21–31. DOI: 10.1016/j.jmps.2019.03.021.
- [25] Rinehart, J.S., 1951, Some quantitative data bearing on the scabbing of metals under explosive attack, *Journal of Applied Physics*, 22, pp.555. <https://doi.org/10.1063/1.1700005>.
- [26] Jung J., 1979, Stress-Wave Grading Techniques On Veneer Sheets, General Technical Report FPL-27, US. Department of Agriculture, Forest Products Laboratory, 1979. available online <https://www.fpl.fs.fed.us/documnts/fplgtr/fplgtr27.pdf>.
- [27] Hascoët E., Herrmann H.J., & Loreto V., 1999, Shock propagation in a granular chain, *The American Physical Review E*, 59, No 3, pp 3202-3206. DOI: 10.1103/PhysRevE.59.3202.
- [28] Boaratti M.F.G. & Ting D.K.S., 2005, International Nuclear Atlantic Conference (INAC 2005), Santos, SP, Brazil, August 28 to September 2, 2005, ABEN, ISBN: 8599141015.
- [29] Sharma M. D., 2007, Effect of initial stress on reflection at the free surface of anisotropic elastic medium, *Journal of Earth System Science*, 116, pp. 537-551, DOI:10.1007/S12040-007-0049-8.
- [30] Cao Z., Liang N., Zeng S., & Gang X., 2022, Dynamic Response Analysis of the Impact Force of Steel Wheel on the Elastic Half-Space, *Jordan Journal of Mechanical and Industrial Engineering*, 16(1), pp. 53 – 62.
- [31] Yousuf L., 2019, The Effect of Temperature on the Stresses Analysis of Composites Laminate Plate, *Jordan Journal of Mechanical and Industrial Engineering*, 13(4), pp. 265 – 269.
- [32] Ali M., 2016, Synthesis and Characterization of Epoxy Matrix Composites Reinforced with Various Ratios of TiC, *Jordan Journal of Mechanical and Industrial Engineering*, 10(4), pp. 231 – 237.
- [33] Suresh S., Giannakopoulos A.E., & Alcalá J., 1997, Spherical indentation of compositionally graded materials: Theory and Experiments, *Acta Materialia*, 45 (4), pp.1307-1321. DOI: 10.1016/S1359-6454(96)00291-1.
- [34] Suresh S., 2001, Graded materials for resistance to contact deformation and damage, *Science*, 292 (5526), pp. 2447-2451. DOI: 10.1126/science.1059716.
- [35] Li Y., Ramesh K.T., & Chin E.S.C., 2001, Dynamic characterization of layered and graded structures under impulsive loading, *International Journal of Solids and Structures*, 38 (34-35), pp. 6045-6061. DOI:10.1016/S0020-7683(00)00364-4.
- [36] Han X., Liu G.R., & Lam K.Y., 2001, Transient Waves in Plates of Functionally Graded Materials, *International Journal for Numerical Methods in Engineering*, 52(8) pp 851-865. <https://doi.org/10.1002/nme.237>.
- [37] Berzovski A., Engelbrecht J., & Maugin G.A., 2003a, Numerical simulation of two-dimensional wave propagation in functionally graded materials, *European journal of mechanics-A/solid*, 22 (2), pp.257-265. [https://doi.org/10.1016/S0997-7538\(03\)00029-9](https://doi.org/10.1016/S0997-7538(03)00029-9).
- [38] Berzovski A., Engelbrecht J., Maugin G.A., 2003b, Stress wave propagation in functionally graded materials, WCU 2003, Paris, September 7-10, pp. 507-509. Corpus ID: 55589577, <http://www.conforg.fr/wcu2003/procs/cd1/articles/000101.pdf>.
- [39] Towfighi, S., Kundu, T., & Ehsani, M. (2002). Elastic wave propagation in circumferential direction in anisotropic cylindrical curved plates. *Journal of Applied Mechanics, Transactions ASME*, 69(3), 283-291. <https://doi.org/10.1115/1.1464872>.
- [40] Taşdemirci A., Hall I.W., Bazle A., Gama B.A., & Güden M., 2004, The Effects of Layer Constraint on Stress Wave Propagation in Multilayer Composite Materials, Army Research Laboratory, ARL-CR 550, available online at https://pdfs.semanticscholar.org/31ee/bc7281a310f64acfeeb6467bc9442b93a4ac.pdf?_ga=2.170619689.825782730.1574531385-1510146761.1566846515. Accessed 23/11/2019.

- [41] Xu L.R., & Rosakis A.J., 2005, Impact Damage Visualization of Heterogeneous Two Layer Materials Subjected to Low Speed Impact, *International Journal of Damage Mechanics*, 14(3), pp. 215 – 223. DOI:10.1177/1056789505048604.
- [42] Gebbeken N. & Greulich S., 2005, Effects of Stress Wave Propagation in Reinforced Concrete Bond considering Crack Opening. *EUROMECH Colloquium 460, Numerical Modelling of Concrete Cracking*, Innsbruck, Austria.
- [43] Zhang G.M., & Batra R.C., 2007, Wave Propagation In Functionally Graded Materials by Modified Smoothed Particle Hydrodynamics (MSPH) Method, *Journal of Computational Physics*, 222 (1), pp. 374- 390, DOI: 10.1016/j.jcp.2006.07.028.
- [44] Perez F. Jr. & Al-Haik M., 2009, Analysis of elastic stress wave propagation through a complex composite structure, *International Journal of Theoretical and Applied Multiscale Mechanics*, 1(2), pp.164–175. DOI:10.1504/IJTAMM.2009.029216.
- [45] Ogden R.W. & Singh B., 2011, Propagation of waves in an incompressible transversely isotropic elastic solid with initial stress: Biot revisited, *Journal of Mechanics of Materials and Structures*, 6 (1-4), pp 453-477. <https://msp.org/jomms/2011/6-1/jomms-v6-n1-p28-p.pdf>.
- [46] Barzkar A. & Adibi H. 2015, On the Propagation of Longitudinal Stress Waves in Solids and Fluids by Unifying the Navier-Lame and Navier-Stokes Equations, *Mathematical Problems in Engineering*, Volume 2015, Article ID 789238, pp. 1-9, <http://dx.doi.org/10.1155/2015/789238>.
- [47] Ebrahim F., Hosseini S. H. S., & Singhal A., 2020, A comprehensive review on the modeling of smart piezoelectric nanostructures, *Structural Engineering and Mechanics*, 74 (5), pp 611-633, DOI: <https://doi.org/10.12989/sem.2020.74.5.611>.
- [48] Ebrahimi, F., Karimiasl, M. & Singhal, A., 2021, Magneto-electro-elastic analysis of piezoelectric–flexoelectric nanobeams rested on silica aerogel foundation. *Engineering with Computers*, 37, pp 1007–1014. <https://doi.org/10.1007/s00366-019-00869-z>.
- [49] Singhal A., Sahu S. A., Nirwal S., & Chaudhary S., 2019, Anatomy of flexoelectricity in micro plates with dielectrically highly/weakly and mechanically compliant interface, *Materials Research Express*, 6, 105714, <https://doi.org/10.1088/2053-1591/ab3f52>.
- [50] Singhal A., Sahu S. A., Chaudhary S., & Baroi J., 2019, Initial and couple stress influence on the surface waves transmission in material layers with imperfect interface, *Materials Research Express*, 6, 105713, <https://doi.org/10.1088/2053-1591/ab40e2>.
- [51] Saroj P. K., Sahu S. A., Singhal A., & Abo-Dahab S. M., 2019, On the transference of Love-type waves in pre-stressed PZT-5H material stick on SiO₂ material with irregularity, *Materials Research Express*, Volume 6, Number 12, DOI: 10.1088/2053-1591/ab5544.
- [52] Timoshenko S., & Goodier J.N., 1951, *Theory of Elasticity*, McGraw-Hill, 2nd ed. New York.

Appendix

A summary of the most related theoretical analysis of the stress wave propagation problem in long bars as well as the elastic impact of spheres is presented [3,18].

The propagation of a compressive pulse in uniform long bars

In a stationary uniform isotropic bar, which is to transmit a longitudinal compressive pulse. Let u denote the displacement of a typical plane, originally distant x from a reference point O. Then $(u + \frac{\partial u}{\partial x} \partial x)$ denotes displacement of a parallel plane, initially at a distant $(x + \partial x)$ from a reference point O. The equation of motion for an element of the bar of initial cross section A_0 is

$$-\frac{\partial \sigma_0}{\partial x} \partial x A_0 = A_0 \rho_0 \partial x \frac{\partial^2 u}{\partial t^2}$$

$$\frac{\partial \sigma_0}{\partial x} = -\rho_0 \frac{\partial^2 u}{\partial t^2} \quad (1)$$

Where, ρ_0 is the density of the material in its unstrained state. The strain in an element of length ∂x is $\frac{\partial u}{\partial x}$. Thus $-\frac{\sigma_0}{\partial u / \partial x} = E$, where E is Young's Modulus.

Thus, differentiating we get,

$$\frac{\partial \sigma_0}{\partial x} = -E \frac{\partial^2 u}{\partial x^2} \quad (2)$$

And using this in Eq. (1) and after rearranging, one can find that:

$$\frac{\partial^2 u}{\partial t^2} = C_L^2 \frac{\partial^2 u}{\partial x^2} \quad (3)$$

Where, $C_L = \sqrt{E/\rho_0}$ is the Longitudinal stress wave speed.

A general solution for Eq. (3) is in the form

$$u = f(x - ct) + F(x + ct)$$

Where f and F are independent arbitrary functions. This is called the D'Alembert solution of the one-dimensional wave equation. The functions f and F describe waves that propagate in the positive and negative x directions with constant velocity or wave speed c , [2].

The propagation of a tensile pulse in non-uniform long bars

In a stationary non-uniform isotropic rod, which is to transmit a longitudinal tensile pulse. Following the known analysis given by [3,18], we get the equation of motion for an element as:

$$\left(\sigma + \frac{\partial \sigma}{\partial x} \delta x\right) \left(A + \frac{\partial A}{\partial x} \delta x\right) - \sigma A = A \rho_0 \delta x \frac{\partial^2 u}{\partial t^2}$$

Neglecting the higher order differential term contains $(\delta x)^2$ and rearranging gives:

$$\frac{\partial \sigma}{\partial x} + \frac{\sigma}{A} \frac{\partial A}{\partial x} = \rho_0 \frac{\partial^2 u}{\partial t^2} \quad (4)$$

Recall that the strain in an element of length ∂x is $\frac{\partial u}{\partial x}$.

Thus,

$$E = \frac{\sigma}{\partial u / \partial x} \quad (5)$$

Differentiating,

$$\frac{\partial \sigma}{\partial x} = E \frac{\partial^2 u}{\partial x^2}$$

And using this in Eq. (4) and after rearrangement and manipulation, one can get:

$$\frac{\partial^2 u}{\partial x^2} + \left(\frac{1}{A} \frac{\partial A}{\partial x}\right) \frac{\partial u}{\partial x} = \frac{\rho_0}{E} \frac{\partial^2 u}{\partial t^2} \quad (6)$$

If the cross-sectional area of the bar is uniform, this equation reduces to Eq. (3) shown above.

$$\frac{\partial^2 u}{\partial t^2} = C_L^2 \frac{\partial^2 u}{\partial x^2}$$

The stress transmission in bars having a discontinuity in cross-sectional area and for bars composed of different materials

Consider an incident elastic wave of compressive stress of intensity σ_I moving through a stationary bar of material S_1 of cross-sectional area A_1 we note, this is partly reflected and partly transmitted at the surface of discontinuity, where another bar of material S_2 of cross-sectional area A_2 is perfectly attached to S_1 [3,18].

The stress wave transmitted through S_2 of intensity σ_T and that reflected back through S_1 , σ_R may be found with the aid of equations, $\sigma_0 = E \vartheta_0 / C_L$ and $\sigma_0 = \rho_0 C_L \vartheta_0$. Bearing in mind that the conditions to be satisfied at the surface of discontinuity are:

The forces on plane surface of discontinuity acting from S_1 and S_2 are always equal, and

The particle velocity in this plane, in material, for S_1 and S_2 , are equal.

If both σ_R and σ_T are taken to be compressive, then,

$$A_1(\sigma_I + \sigma_R) = A_2 \sigma_T \quad (7)$$

And noting that σ_I and σ_R are associated with waves travelling in opposite directions, therefore (b) gives,

$$V_I - V_R = V_T \quad \text{or} \quad (8)$$

$$\sigma_I - \sigma_R = \sigma_T$$

Where V denote particle speed and subscripts I, R and T refer to incident, reflected and transmitted stresses. Hence,

$$\sigma_T = \frac{2A_1 \rho_2 C_2}{A_1 \rho_1 C_1 + A_2 \rho_2 C_2} \sigma_I \quad (9)$$

And

$$\sigma_R = \frac{A_2 \rho_2 C_2 - A_1 \rho_1 C_1}{A_1 \rho_1 C_1 + A_2 \rho_2 C_2} \sigma_I \quad (10)$$

From Eq. (9) note that for simple change in cross-sectional areas, i.e. when S_1 and S_2 are of the same material and $\rho_1 = \rho_2$ and $C_1 = C_2$, the incident and reflected waves have the same or opposite signs according to the increase or decrease in size of the cross sectional area; and at the same time the intensity of the transmitted stress falls below or exceeds the intensity of the incident stress.

Eqs. (9) and (10) are approximate since the derivations are based on some simplifying assumptions; and at the discontinuity, condition (b) is true only inside the material, not at the end surfaces. Complicated local stress wave interactions occur in the vicinity of the surface of discontinuity and for a length equal to about the first diameter. Note that for $\rho_1 = \rho_2$ and $E_1 = E_2$ i.e. $C_1 = C_2$

If $A_2/A_1 \rightarrow 0$, i.e. the end of the rod is effectively free and the above equations give $\sigma_R \rightarrow -\sigma_I$ and $\sigma_T \rightarrow 2\sigma_I$, and

If $A_2/A_1 \rightarrow \infty$, i.e. the end of the rod is effectively fixed, $\sigma_R \rightarrow \sigma_I$ and $\sigma_T \rightarrow 0$.

Eqs. (9) and (10) show that a small shaft on the end of one larger in cross-sectional area can act as a wave (or momentum) trap to a pulse or blow on the far end of the larger shaft.

For no wave to be reflected from the discontinuity in the bar, it is required that $\sigma_R = 0$, and then $A_1 \rho_1 C_1 = A_2 \rho_2 C_2$, i.e. impedance matching. So that:

$$\sigma_T = \sigma_I \cdot \sqrt{\frac{E_2 \rho_2}{E_1 \rho_1}} \quad (11)$$

The central elastic impact of sphere

Following the well-known Hertz analysis of two spheres undergone simple elastic impact. The equation of motion for each sphere is given by

$$m_1 \frac{dV_1}{dt} = -P \text{ and } m_2 \frac{dV_2}{dt} = -P \quad (12)$$

Let x be the distance through which the two spheres approach by virtue of local compression.

$$\frac{dx}{dt} = V_1 + V_2 \quad (13)$$

After differentiating and using Eq. (12), one can find that:

$$\frac{\partial^2 x}{\partial t^2} = -P \left(\frac{m_1 + m_2}{m_1 \cdot m_2} \right) \quad (14)$$

Let, $\mu = \frac{m_1 + m_2}{m_1 \cdot m_2}$, then

$$\frac{\partial^2 x}{\partial t^2} = -\mu P \quad (15)$$

Timoshenko and Goodier [52] give that

$$P = Kx^{3/2} \quad (16)$$

where,

$$K = \frac{4}{3\pi \left[\frac{1-\theta_1^2}{\pi E_1} + \frac{1-\theta_2^2}{\pi E_2} \right]} \left(\frac{R_1 \cdot R_2}{R_1 + R_2} \right)^{1/2} \quad (17)$$

And θ denotes Poisson's ratio. Substituting Eq. (17) into Eq. (16) and integrating gives:

$$\frac{1}{2} (x^2 - V_0^2) = -\frac{2}{5} K \mu x^{5/2} \quad (18)$$

Where $V_0 = V_1 + V_2$ when $t = 0$,

For maximum compression, x_0 , the velocity \dot{x} is zero; Thus

$$x_0 = \left(\frac{5V_0^2}{4K\mu} \right)^{2/5} \quad (19)$$

From Eq. (18) and after rearrangement, one can get:

$$\frac{dx}{dt} = V_0 \left[1 - \left(\frac{x}{x_0} \right)^{5/2} \right]^{1/2}$$

Hence, the time to maximum compression, T , is

$$T = 1.47 \frac{x_0}{V_0} \quad (20)$$

For spherical body impacting against a plane surface, i.e. $R_1 \rightarrow \infty$

$$K = \frac{4}{3\pi \left[\frac{1-\theta_1^2}{\pi E_1} + \frac{1-\theta_2^2}{\pi E_2} \right]} (R_2)^{1/2} \quad (21)$$

And time of contact, t , is

$$t = 2T$$